

PROTOSTELLAR COLLAPSE IN A SELF-GRAVITATING SHEET

LEE HARTMANN,¹ ALAN BOSS,² NURIA CALVET,³ AND BARBARA WHITNEY¹

Received 1994 April 5; accepted 1994 May 5

ABSTRACT

We present preliminary calculations of protostellar cloud collapse starting from an isothermal, self-gravitating gaseous layer in hydrostatic equilibrium. This gravitationally unstable layer collapses into a flattened or toroidal density distribution, even in the absence of rotation or magnetic fields. We suggest that the flat infalling envelope recently observed in HL Tau by Hayashi et al. is the result of collapse from an initially nonspherical layer. We also speculate that the later evolution of such a flattened, collapsing envelope can produce a structure similar to the “flared disk” invoked by Kenyon and Hartmann to explain the infrared excesses of many T Tauri stars.

Subject headings: accretion, accretion disks — stars: formation — stars: pre-main-sequence

1. INTRODUCTION

Most models for the formation of low-mass stars from molecular material start with an initially spherically symmetric cloud (e.g., Larson 1972; Appenzeller & Tscharnuter 1974; Shu 1977; Bodenheimer & Black 1978; Boss 1980; Terebey, Shu, & Cassen 1984, hereafter TSC). Although this assumption is generally made for simplicity rather than realism, such models have been successful in explaining several observational features of the heavily extincted, low-luminosity “Class I” young stellar objects (“protostar” candidates; Lada & Wilking 1984). For example, the predicted timescale during which the central protostar is heavily obscured by its dusty infalling envelope is consistent with source counts in the Taurus molecular cloud (Myers et al. 1987; Kenyon et al. 1990; Beichman et al. 1992; Kenyon et al. 1994). In addition, the collapse models of TSC, which are spherical on large scales but flattened on small scales due to rotation, can produce dust emission that matches the mid- to far-infrared spectra of many Class I sources (Adams, Lada, & Shu 1987; Butner et al. 1991; Butner, Natta, & Evans 1994; Kenyon, Calvet, & Hartmann 1993a; Kenyon et al. 1993b).

Despite the successes of initially spherical collapse models, there are reasons to consider departures from sphericity on large scales. The near-infrared fluxes, scattered light images, and polarization properties of many heavily extincted young stellar objects cannot be explained with simple TSC models, but require some kind of “hole” in the dusty envelope to permit more short-wavelength light to escape (Whitney & Hartmann 1993; Kenyon et al. 1993b). Although bipolar outflows are very likely to drive holes in infalling envelopes (e.g., Shu, Adams, & Lizano 1987), protostellar jets seem much more highly collimated than the apparent large opening angles of many reflection nebulae (see, e.g., Mundt, Ray, & Bührke 1988; Kepner et al. 1993). Alternatively, a “hole” or path of lower optical depth with a relatively large “opening angle” could be

produced if the surrounding dusty envelope is not spherical but flattened on large scales.

Recently Hayashi, Ohashi, & Miyama (1993) interpreted the ¹³CO emission around the heavily extincted T Tauri star HL Tau (cf. Sargent & Beckwith 1987, 1991) in terms of an infalling, flattened “disk” of radial dimensions ~1400 AU. The flattening of this disk appears to be inconsistent with the TSC model, although the observations might be reconciled with collapse of an initially spherical cloud whose dynamics are affected by a modest magnetic field (Galli & Shu 1993a, b).

Apart from simplicity there is really no reason to require sphericity of the initial star-forming cloud. Observations of molecular cloud cores thought to be the precursors of low-mass stars suggest that they are elongated in approximately a 2:1 ratio (Myers et al. 1991), and if the elongation reflects an initially prolate cloud, binary fragmentation may result (Boss 1993). From a broader perspective, several investigators (Larson 1985; Bonnell & Bastien 1992; Bonnell et al. 1992) have suggested that the fragmentation required to make binary or multiple star systems is most naturally accomplished in sheetlike or filamentary cloud geometries, for which there is ample observational evidence (Schneider & Elmegreen 1979). Magnetic support might also result in an initially flattened cloud (e.g., Mouschovias 1976). Collapse from such structures might well depart substantially from spherical symmetry (see, e.g., Miyama, Narita, & Hayashi 1987).

In this *Letter* we present an initial investigation of flattened infalling envelopes. For concreteness we consider the collapse of an isothermal, self-gravitating sheet in the absence of magnetic fields. Further numerical calculations and observational predictions of this picture will be presented in forthcoming papers.

2. ASSUMPTIONS

2.1. Initial Conditions

We consider sheetlike initial conditions rather than filaments for simplicity, although filamentary structures may generally result from sheet fragmentation (Miyama et al. 1987). An isothermal, infinite, self-gravitating, flat layer, symmetric about the $z = 0$ plane, has density distribution given by

$$\rho(z) = \rho(0) \operatorname{sech}^2(z/H), \quad (1)$$

¹ Harvard-Smithsonian Center for Astrophysics, 60 Garden Street, Cambridge, MA 02138. Electronic mail: hartmann@cfa.harvard.edu, bwhitney@cfa.harvard.edu

² DTM, Carnegie Institution of Washington, 5241 Broad Branch Road, NW, Washington, DC 20015-1305. Electronic mail: boss@ciw.ciw.edu

³ Centro de Investigaciones de Astronomía, Ap. Postal 264, Mérida 5101A, Venezuela. Electronic mail: calvet@cida.uunet.ve

where the scale height is defined by

$$H = c_s^2/(\pi G \Sigma), \quad (2)$$

where c_s is the isothermal sound speed and Σ is the total surface density (Spitzer 1978). For this density distribution, modes of the form $\cos kx$ or $J_0(kr)$ are gravitationally unstable for wavenumbers $k_c \leq H^{-1}$. Following Larson (1985), we define a critical mass as the mass interior to the first minimum of the Bessel function with the critical wavenumber,

$$M_c = 4.67 c_s^4 / (G^2 \Sigma). \quad (3)$$

To fix ideas, consider a slab with $T = 10$ K, comparable to temperatures estimated in the Taurus molecular cloud, and a mean molecular weight of $2m_H$. The for $M_c = 1 M_\odot$, $\Sigma = 9.1 \times 10^{-2} \text{ g cm}^{-2}$; the scale height is $H = 1440$ AU, and the central density $\rho(0) = 2.12 \times 10^{-18} \text{ g cm}^{-3}$. For a typical interstellar medium opacity law (Draine & Lee 1984), the surface density implies a visual extinction perpendicular through the sheet of $A_V = 15$, comparable to the $A_V \sim 10^1$ estimated for Taurus molecular cloud cores (Myers & Benson 1983; Cernicharo, Guelin, & Askne 1984). One solar mass is contained in a sphere (centered on $z = 0$) of diameter $\sim 1.72 \times 10^{17} \text{ cm} \sim 1.15 \times 10^4 \text{ AU}$, which is slightly larger than the critical wavelength $\lambda = 2\pi/k_c = 0.89 \times 10^4 \text{ AU}$. The radial dimension of this $1 M_\odot$ layer is only about a factor of 2 smaller than the outer radius $R = 10^4 \text{ AU}$ of a critical isothermal sphere of $1 M_\odot$ at 10 K (cf. Shu 1977). However, the vertical scale height of our density distribution is substantially smaller.

2.2. Methods for Hydrodynamic Calculations

We use the spatially and temporally second-order-accurate hydrodynamics code described by Boss & Myhill (1992). The code computes the self-gravitational hydrodynamics of a gas cloud inside a spherical volume on an (r, θ, ϕ) grid. For our initial exploration we consider only axisymmetric ($\partial/\partial\phi = 0$) modes. Material exterior to the spherical outer boundary is not allowed to pass through the spherical boundary, but the gravity of the entire infinite sheet is taken into account, so that the initial self-gravitating layer is in hydrostatic equilibrium. The external field was calculated by subtracting the initial gravitational potential of the matter inside the spherical grid from the potential of the infinite sheet. While the code geometry is not naturally suited to this problem, the use of a nonuniform θ grid with grid points concentrated at the midplane provides ample spatial resolution in the densest regions. Further, our calculations maintain the initial equilibrium configuration for a few free-fall times.

The initial cloud is marginally unstable to collapse (cf. § 2.1). No specific perturbation leading to collapse is employed beyond that of the geometry of the grid. Since we are more interested in the structure of the infalling envelope than the central protostellar core, we ignore the protostellar regions; the innermost cell has a radius of ~ 7 AU. We assume a flow-through boundary condition at that radius so that the central cell acts as a “sink cell” (Boss & Black 1982) whose mass is a point source of gravity. Once the protostellar core forms, we switch to a free-fall inner boundary condition on the radial component of the velocity field.

Timescales are reported in terms of the reference spherical free-fall time for the initial midplane density, $t_{\text{ff}} = [3\pi/32G\rho(0)]^{1/2} = 4.6 \times 10^4 \text{ yr}$.

3. RESULTS

In Figures 1a–1d we present density contours and velocity fields for the hydrodynamic model at representative times during the collapse. The initial model is close to hydrostatic equilibrium, with maximum velocities $\sim 1 \text{ cm s}^{-1}$. Appreciable motions develop around $t \sim 2.7t_{\text{ff}}$, when the upper regions of the envelope begin moving at substantial but subsonic maximum velocities $\sim 0.13 \text{ km s}^{-1}$ (Fig. 1a). Even at this point the material in the central layer is moving much more slowly, with motions largely parallel to the midplane. This apparently occurs because the gas pressure gradient suppresses motion more effectively in the vertical direction, while there is no initial pressure gradient in the horizontal direction. Material then begins to pile up along the central axis, and then falls in, leaving behind a relatively evacuated axial region.

The collapse does not really get going until $t \gtrsim 5t_{\text{ff}}$, when maximum velocities become supersonic and a central core begins to develop (Figs. 1b–1d). Once an appreciable mass builds up in the central region ($t \gtrsim 6t_{\text{ff}}$) the flow becomes nearly radial. By $t \sim 6t_{\text{ff}}$, the central core has a mass of $\sim 0.15 M_\odot$, and the infall rate to the core has reached $\sim 3 \times 10^{-5} M_\odot \text{ yr}^{-1}$ (Fig. 2). At $t \sim 7t_{\text{ff}}$, the central core has a mass $\sim 0.65 M_\odot$ and the infall rate has leveled off to $\sim 6 \times 10^{-6} M_\odot \text{ yr}^{-1}$; at this point 35% of the mass remains in the envelope.

Calculations with a constant density outer boundary condition indicate that the decrease in infall seen at $t \gtrsim 7.5t_{\text{ff}}$ (Fig. 2) is due to the non-flow-through outer boundary condition. This is roughly one sound crossing time after the central mass begins to grow. We therefore feel that our results at earlier times for the inner regions are not very dependent upon the boundary conditions. (The outermost regions exhibit a corresponding decrease in density sooner; see Fig. 1b.) The outer boundary condition should not affect our general result of a flattened collapse, with a relatively evacuated polar region, since there is very little exterior mass than can be accreted in polar directions (the outer boundary lies ~ 4 scale heights above the midplane). The assumption of a limited amount of accretable mass in the plane of the layer may be realistic if several stars are forming from the fragmenting sheet. Then material external to our calculational volume might not flow in, but rather fall toward other mass centers.

Our results show that (a) collapse from a self-gravitating sheet results in a flattened infalling envelope, with the flattening increasing with time (cf. Miyama et al. 1987); and (b) there is an evacuated region along the central axis, suggestive of a bipolar outflow cavity, but produced without an outflow. Our assumption of axisymmetry in effect specifies the location of the ultimate mass concentration, and makes the central axis a special location, so the details of our results may not be applicable to the general problem of collapse in a sheet. The qualitative result that less material is present near the central axis is likely to be robust since the infalling material should tend to fall in first along the shortest distance (the central axis) once the central mass has grown sufficiently that its gravity dominates gas pressure forces. In addition, the inclusion of modest rotation would also tend to make an axial reduction in density by forcing material to land on a disk at a finite distance from the central object (see, e.g. TSC; Boss 1987).

4. DISCUSSION

In the standard model (e.g., Shu et al. 1987), collapse proceeds from an initial spherical cloud in pressure equilibrium.

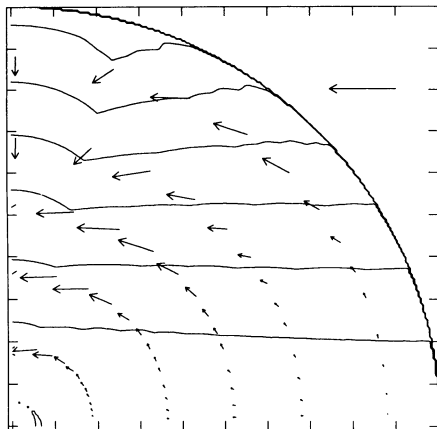


FIG. 1a

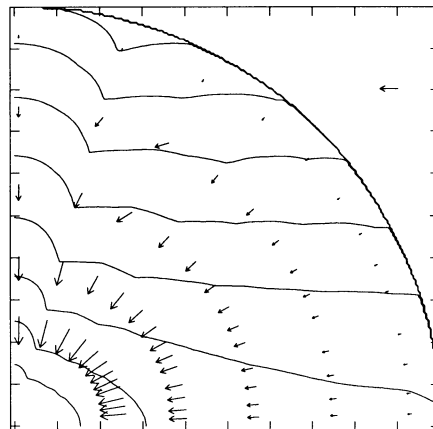


FIG. 1b

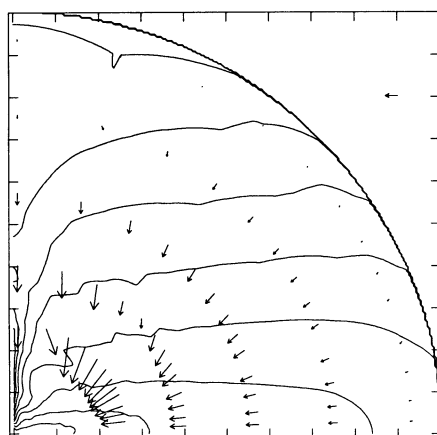


FIG. 1c

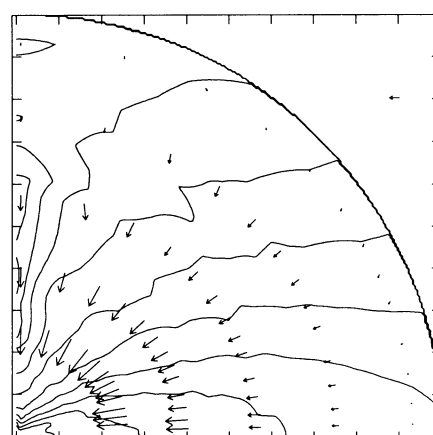


FIG. 1d

FIG. 1.—Velocity fields and density contours separated by factors of $10^{1/2}$ at selected times for the collapse model described in the text: (a) $t = 2.7t_{\text{ff}}$; (b) $t = 6.0t_{\text{ff}}$; (c) $t = 6.5t_{\text{ff}}$; (d) $t = 7.0t_{\text{ff}}$. The left-hand border is the symmetry axis; the bottom border is $z = 0$. The entire cloud is shown (radius = 5400 AU). The r and θ grids are nonuniform and resolve the cloud outside 7 AU (not visible here). The highest (central) density contours denote a molecular hydrogen number density of $3.16 \times 10^6 \text{ cm}^{-3}$ in all except (a), where the highest contour is $3.16 \times 10^5 \text{ cm}^{-3}$. Velocity vectors are plotted for only a small fraction of the $50 \text{ radial} \times 22 \text{ angular}$ grid points. The lengths of the velocity vectors are proportional to the speeds, with the length of the arrow in the upper right-hand corner denoting the sound speed = 0.2 km s^{-1} .

The collapse tends to be “inside-out,” since the higher density central regions will collapse first. Neglecting magnetic fields, the mass infall rate is dependent only on the sound speed, $\dot{M} \sim M/t_{\text{ff}} \sim c_s^3/G$ (cf. Shu 1977), and is nearly constant in time (Shu 1977; Boss & Black 1982); for $T = 10 \text{ K}$, $\dot{M} \sim 2 \times 10^{-6} M_{\odot} \text{ yr}^{-1}$.

The collapse of the flat layer produces somewhat different results. Because there is a minimum wavelength for the initial gravitational instability, we do not get a pure “inside-out” collapse, even though we have specified the location of the central mass by the assumption of axial symmetry. Our “plateau” phase infall rate $\sim 6 \times 10^{-6} M_{\odot} \text{ yr}^{-1}$ (Fig. 2) is somewhat higher than that for isothermal sphere collapse at 10 K, but is in reasonable agreement with typical estimates $\dot{M} \sim 4 \times 10^{-6} M_{\odot} \text{ yr}^{-1}$ for Taurus Class I (embedded) sources (Adams et al. 1987; Kenyon et al. 1993a, b).

In our collapsing layer, the polar regions fall in before the equatorial regions. This can produce a relatively evacuated polar “cavity” in the absence of any bipolar outflow (Fig. 1d; also Boss 1987). Jets will probably affect the density distribution in the polar regions, but the apparent “opening angle” of the dusty nebula, detected in scattered light (cf. Whitney &

Hartmann 1993), may represent the structure of the flattened infall rather than the geometry of the jet.

This picture of a collapsing “thick disk” or toroid may explain the infalling envelope of HL Tau. Hayashi et al. (1993; Lin et al. 1994) estimate an infall rate for the disk of HL Tau $\sim 0.5 \times 10^{-5} M_{\odot} \text{ yr}^{-1}$ at a radius of $\sim 1400 \text{ AU}$. In our model, at a time of $t = 7t_{\text{ff}}$, the infall rate is $\sim 0.7 \times 10^{-5} M_{\odot} \text{ yr}^{-1}$, comparable to other estimates of infall in HL Tau derived from studies of scattered light (Beckwith et al. 1989), redshifted C_2 absorption lines (Grasdalen et al. 1989), and analysis of the far-infrared emission (Calvet et al. 1994).

In Figure 3 (Plate L5) we show some simple velocity channel maps of the model at $t = 7t_{\text{ff}}$, assuming that the emission is linearly proportional to the surface density. The model is viewed at an inclination angle of 60° to produce a flattened distribution of gas similar to that observed in HL Tau. The pattern of these channel maps, with a velocity gradient along the minor axis of the projected gas distribution, and with the highest velocities confined to regions near the center, qualitatively resemble the channel maps of HL Tau obtained by Hayashi et al. (1993) (see also Sargent & Beckwith 1987, 1991). On small scales, the observations suggest rotation which is not

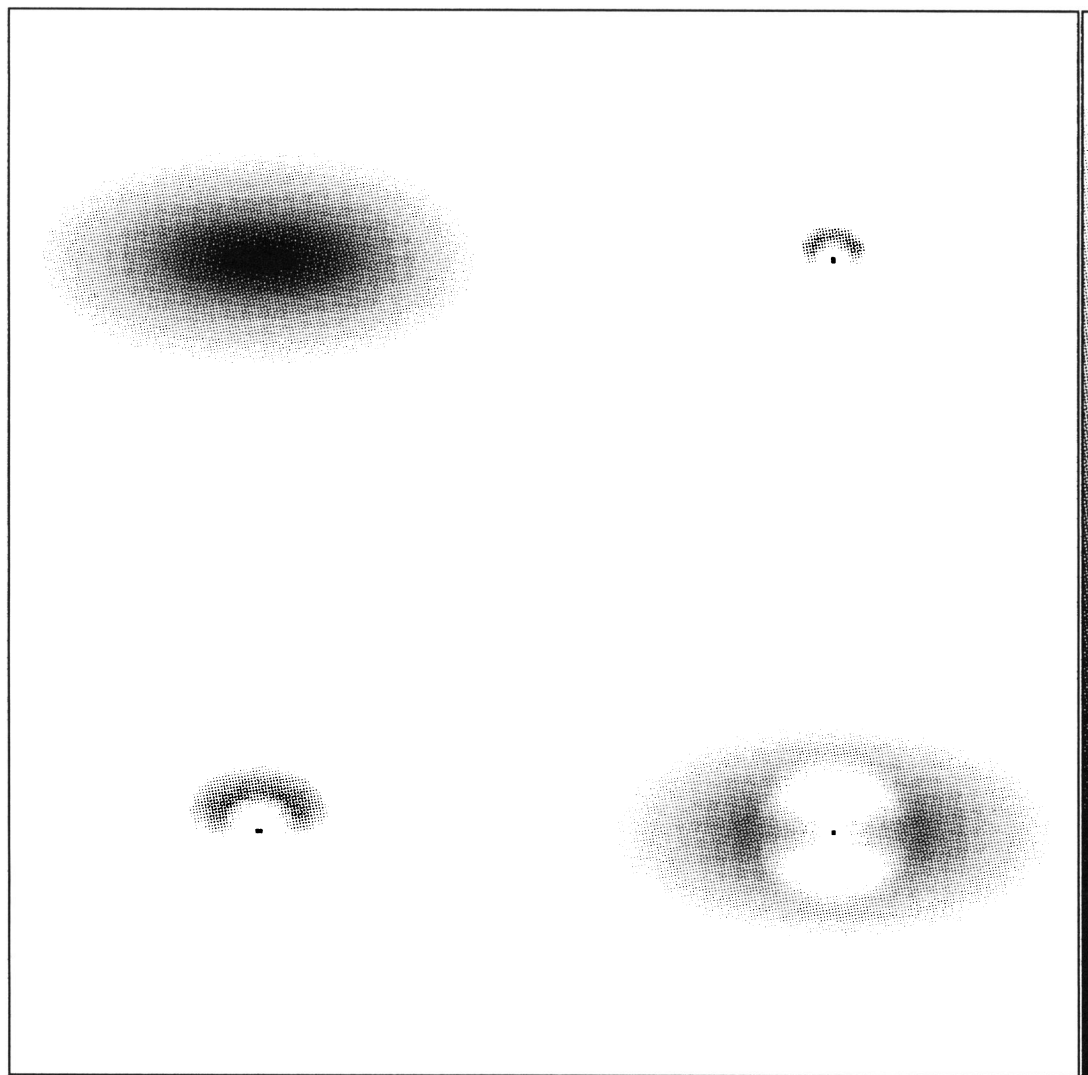


FIG. 3.—Maps of the surface density within different projected velocity ranges for the infall model at $t = 7.0t_{ff}$, observed at an inclination angle of the symmetry axis to the line of sight of 60° . The intensities are on a linear scale, with the lowest surface density displayed = 0.01 g cm^{-2} , and the highest being = 0.2 g cm^{-2} . In all plots the upper portion of the figure corresponds to the region of the envelope farthest away from the observer, with the dot indicating the central point (*star*). The upper left-hand panel corresponds to $-5 \text{ km s}^{-1} \leq v \leq 5 \text{ km s}^{-1}$; the upper right, $-0.75 \text{ km s}^{-1} \leq v \leq -0.5 \text{ km s}^{-1}$; the lower right, $-0.5 \text{ km s}^{-1} \leq v \leq -0.25 \text{ km s}^{-1}$; and the lower left panel, $-0.25 \text{ km s}^{-1} \leq v \leq 0.25 \text{ km s}^{-1}$.

HARTMANN et al. (see 430, L51)

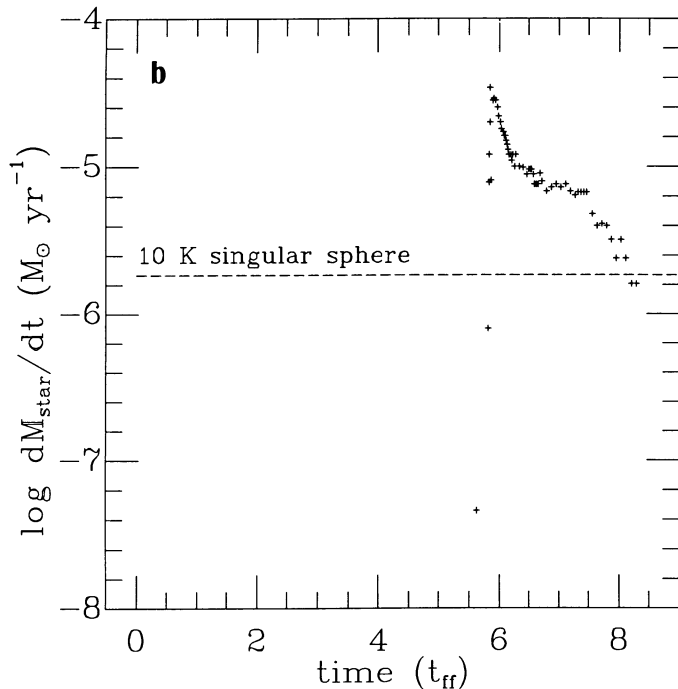


FIG. 2.—Mass accretion rate of the central protostar (sink cell of radius of 7 AU) as a function of time.

included in our model; we expect that the introduction of a modest amount of rotation in the outer envelope, which would not affect the motion on large scales, would produce sufficiently rapid rotation in the inner regions.

The models also suggest that the infalling envelope will become increasingly flattened as the collapse proceeds. At later times the density distributions are reminiscent of the “flared disks” invoked by Kenyon & Hartmann (1987) to explain the

far-infrared excesses of many T Tauri stars. To indicate the flatness of the density distribution, we consider visual optical depths to the central star as a function of inclination angle. The actual optical depth in the model is sensitive to the arbitrary size of the inner boundary. To avoid this difficulty we compute only the optical depths into a radius of 100 AU; the angular momentum of the infalling matter might well prevent material from coming closer than this (see, e.g., TSC; Kenyon et al. 1993a, b). Again using the Draine & Lee (1984) opacities, we find $A_v \sim 50$ at $\cos i = 0.1$ while $A_v \sim 1.5$ at $\cos i = 0.9$ (at $t = 7t_{ff}$). Such optically thick infalling structures could explain the infrared emission of T Tauri stars in excess of that expected from a flat, steady disk, perhaps even for much lower infall rates (Natta 1993).

Galli & Shu (1993a, b) showed that collapse from a spherical cloud may still result in flattened infall if a magnetic field is present. While this is quite possible, our results show that it is not necessary to invoke magnetic effects if the initial cloud is not spherical.

Since real clouds are not infinite self-gravitating layers, our calculations may represent a limiting case. The typical situation may be intermediate between our sheet assumption and the usual spherical model. We are currently calculating infall models with rotation and with different surface densities. Detailed radiative transfer calculations are underway to test further aspects of this model by comparing with observed SEDs and scattered light fluxes and images of young stellar objects. The results may have implications for the fragmentation of molecular clouds into stars.

We are grateful for thoughtful comments from an anonymous referee. This work was supported in part at CfA by NSF grant INT 92-03015, CONICIT grant PI-078, and by NASA grants NAGW-2306 and NAGW-2919. A. P. B. was partially supported by NSF grant AST 92-17967.

REFERENCES

- Adams, F. C., Lada, C. J., & Shu, F. H. 1987, *ApJ*, 312, 788
 Appenzeller, I., & Tscharnuter, W. 1974, *A&A*, 30, 423
 Beckwith, S. V. W., Sargent, A. I., Koresko, C. D., & Weintraub, D. A. 1989, *ApJ*, 343, 393
 Beichman, C. A., Boulanger, F., & Moshir, M. 1992, *ApJ*, 386, 248
 Bodenheimer, P., & Black, D. C. 1978, in *Protostars and Planets*, ed. T. Gehrels (Tucson: Univ. of Arizona Press), 288
 Bonnell, I., Arcoragi, J. P., Martel, H., & Bastien, P. 1992, *ApJ*, 400, 579
 Bonnell, I., & Bastien, P. 1992, *ApJ*, 401, 654
 Boss, A. P. 1980, *ApJ*, 237, 563
 ———. 1987, *ApJ*, 316, 721
 ———. 1993, *ApJ*, 410, 157
 Boss, A. P., & Black, D. C. 1982, *ApJ*, 258, 270
 Boss, A. P., & Myhill, E. A. 1992, *ApJS*, 83, 311
 Butner, H. M., Evans, N. J., II, Lester, D. F., Levreault, R. M., & Strom, S. E. 1991, *ApJ*, 376, 676
 Butner, H. M., Natta, A., & Evans, N. J., II, 1994, *ApJ*, 420, 326
 Calvet, N., Hartmann, L., Kenyon, S., & Whitney, B. 1994, *ApJ*, in press
 Cernicharo, J., Guélin, M., & Askne, J. 1984, *A&A*, 138, 371
 Draine, B. T., & Lee, H. M. 1984, *ApJ*, 285, 89
 Galli, D., & Shu, F. H. 1993a, *ApJ*, 417, 220
 ———. 1993b, *ApJ*, 417, 243
 Grasdalen, G. L., Sloan, G., Stout, M., Strom, S. E., & Welty, A. D. 1989, *ApJ*, 339, L37
 Hayashi, M., Ohashi, N., & Miyama, S. 1993, *ApJ*, 418, L71
 Kenyon, S. J., Calvet, N., & Hartmann, L. 1993a, *ApJ*, 414, 676
 Kenyon, S. J., Gomez, M., Marzke, R., & Hartmann, L. 1994, *AJ*, submitted
 Kenyon, S. J., & Hartmann, L. 1987, *ApJ*, 323, 714
 Kenyon, S. J., Hartmann, L. W., Strom, K. M., & Strom, S. E. 1990, *AJ*, 99, 869
 Kenyon, S. J., Whitney, B., Gomez, M., & Hartmann, L. 1993b, *ApJ*, 414, 773
 Kepner, J., Hartigan, P., Yang, C., & Strom, S. 1993, *ApJ*, 415, L119
 Lada, C. J., & Wilking, B. A. 1984, *ApJ*, 287, 610
 Larson, R. B. 1972, *MNRAS*, 157, 121
 ———. 1985, *MNRAS*, 214, 379
 Lin, D. N. C., Hayashi, M., Bell, K. R., & Ohashi, N. 1994, *ApJ*, in press
 Miyama, S. M., Narita, S., & Hayashi, C. 1987, *Prog. Theoret. Phys.*, 78, 1273
 Mouschovias, T. Ch. 1976, *ApJ*, 207, 141
 Mundt, R., Ray, T. P., & Bührke, T. 1988, *ApJ*, 333, L69
 Myers, P. C., & Benson, P. J. 1983, *ApJ*, 266, 309
 Myers, P. C., Fuller, G. A., Goodman, A. A., & Benson, P. J. 1991, *ApJ*, 376, 561
 Myers, P. C., Fuller, G. A., Mathieu, R. D., Beichman, C. A., Benson, P. J., Schild, R. E., & Emerson, J. P. 1987, *ApJ*, 319, 340
 Natta, A. 1993, *ApJ*, 412, 767
 Sargent, A. I., & Beckwith, S. 1987, *ApJ*, 323, 294
 ———. 1991, *ApJ*, 382, L31
 Schneider, S., & Elmegreen, B. G. 1979, *ApJS*, 41, 87
 Shu, F. H. 1977, *ApJ*, 214, 488
 Shu, F. H., Adams, F. C., & Lizano, S. 1987, *ARA&A*, 25, 23
 Spitzer, L. 1978, *Physical Processes in the Interstellar Medium* (New York: J. Wiley), 283
 Terebey, S., Shu, F. H., & Cassen, P. 1984, *ApJ*, 286, 529 (TSC)
 Whitney, R. A., & Hartmann, L. 1993, *ApJ*, 402, 605